Abbott, A.N., 2019, A benthic flux from calcareous sediments results in non-conservative neodymium behavior during lateral transport: A study from the Tasman Sea: Geology, https://doi.org/10.1130/G45904.1

Supplemental Table DR1

	Site Name	Latitude	Longitude	Water Depth	% Calcareous
Pore Water Sites					
	PH150	**-34.1282**	**151.2362**	**150 m**	**40**
	JB1500	**-34.4976**	**151.2006**	**1550 m**	**45**
	CB2600	**-31.9557**	**153.3034**	**2660 m**	**51**
Water Column Sites					
	CTD23	**-36.8889**	**152.5472**	**4820 m**	**n/a**
	CTD54	**-27.9228**	**155.1451**	**4460 m**	**n/a**

Table DR1: Site locations, water depths, and percent of calcareous sediments. Sediment % carbonate was determined by pressure calcimetry and confirmed by X-ray diffraction (PANalytical Aeris XRD) at Macquarie University.

CB2600 Additional Information

Site CB2600 was located at the base of a submarine canyon along the east coast of Australia (Supplemental Figure DR1). The advection of marine sediments through such submarine canyons has been widely observed (e.g. Schmidt and DeDeckker, 2015) and the large (80-120 μm) grains at CB2600 (Supplemental Figure DR2) are likely due to such events carrying significant amounts of sediment to the canyon floor from shallower environments. These sediment transport events potentially disrupt the upper most sediment column and may result in an advective mixing of the overlying bottom

water with the pore water from the disturbed sediments.

Accessory Pore Water Data

Pore water dissolved iron, manganese, and phosphorous were measured on the Spectros Arcos ICP-OES in the Keck Collaboratory for Plasma Spectrometry at Oregon State University. Dissolved iron was not correlated to dissolved neodymium in the pore water at any of the Tasman Sea sites, nor was manganese or phosphorous (Supplemental Figure DR3). Dissolved iron appeared below the subsurface maximum in

neodymium in the pore water profile at all three sites. Iron was highest (>25 ppb) at PH150 below 12 cm with lower concentrations at both JB1500 and CB2600 (<10 ppb). Iron and manganese were below detection limit (0.310 ppb Fe, 0.013 ppb Mn) in the upper 7 cm at both JB1500 and CB2600. All three Tasman Sea sites had generally low dissolved manganese with the highest measured dissolved manganese was below 9 cm at CB2600. Dissolved phosphorous was measured in all samples and generally showed an increase with depth in the sediment column. Excluding bottom water (depth = 0, Supplemental Figure DR3), the greatest increase in dissolved phosphorous within the pore water profile at a single site was at PH150 (~100 ppb increase).

Seawater REE Patterns

Neodymium (Nd) is one of the rare earth elements (REEs), or lanthanides. Nd is often the focus of paleocirculation studies because the apparent quasi-conservative behavior of neodymium isotopes in the ocean makes the isotopic signature a tracer of water mass origin (e.g. von Blanckenburg, 1999). Because of the implications of non-conservative behaviour of neodymium on paleo-interpretations, this manuscript focuses on the potential influence of a benthic source on the oceanic neodymium budget. However, the largely coherent chemical properties of the lanthanides make the REEs as a series more useful than an individual element in identifying process (e.g. Elderfield and Greaves, 1982). Specifically, understanding how rare earth elements fractionate from one another as a function of solid-fluid interactions (e.g. Censi et al., 2007; Kuss et al., 2001), scavenging (e.g. Bertram and Elderfield, 1993; Nozaki and Alibo, 2003), complexation (e.g. Goldberg et al., 1963; Turner et al., 1981; Akagi, 2013), and dissolution (e.g. Lacan and Jeandel, 2005; Jeandel &

Oelkers, 2015) can supply additional information to constrain the processes that control the REE budget in the ocean. The seawater REE 'patterns' (i.e. the REE concentrations normalised to shale values) from Tasman Sea CTD sites 23 and 54 provide additional evidence for the influence of a benthic flux. The normalisation to shale values removes the naturally occurring odd-even pattern in the REE abundances (Byrne and Sholkovitz, 1996) and a secondary normalisation to praseodymium concentrations allows patterns to be directly compared between samples with dissimilar concentrations. Extensive research has shown that the REE pattern of seawater is characterised by a heavy REE (HREE) enriched pattern with a pronounced negative Ce anomaly (e.g. Goldberg et al., 1963; Elderfield and Greaves, 1982; Klinkhammer et al., 1983; Piepgras and Jacobsen, 1992) and that the REE pattern of pore water is generally less HREE enriched than seawater and may exhibit middle REE (MREE) enrichment, or a 'bulge' in the REE pattern (Elderfield and Sholkovitz, 1987; Sholkovitz et al., 1989; Haley et al., 2004; Schacht et al., 2010; Kim et al., 2012; Abbott et al., 2015a; Du et al., 2016; Haley et al., 2017).

The REE fraction was analysed using a SeaFAST II in line with a Thermo VG ExCell quadrupole ICP-MS at the Keck Collaboratory for Plasma Mass Spectrometry at Oregon State University following the methods of Yang and Haley (2016). A seawater sample (NBP95R10) from 1152 m water depth in the Bransfield Strait (Southern Ocean, 62°46'S, 59°24'W) was used as an in-house consistency standard as no calibrated seawater or pore water REE standards are available (n=16; mean and standard deviation in Supplemental Table 2). The procedural blank was measured on 1% distilled nitric acid run through the ESI SeaFAST II as an unknown sample (blank values reported in Supplemental Table DR2). All REEs are normalised to Post Archaen

Australian Shale (PAAS) after Taylor and McLennan (1985) with the values used for

normalisation reported here in ppm (Supplemental Table DR2).

For this discussion, I group seawater into 5 categories: bottom water, deeper than

3000 m, between 2000 and 3000 m, between 1000 and 2000 m, and shallower than

1000 m (Supplemental Figure DR4). In this case, bottom water is the water

collected from the Niskin bottle triggered closest to the seafloor (within 10 m) and

was processed as discussed in the main text. Note that the bottom water reported for

CB2600 and JB1500 (main text Figure 2) are from a Niskin bottle attached to the

multi-core frame rather than from a CTD cast, meaning those water samples were

collected within a meter of the sediment-water interface. No Niskin bottle attached to

the CTD rosette was lowered to within 5 meters of the sediment-water interface to

protect the instrumentation from contact with the bottom in the case of unexpected

swells.

Supplemental Table DR2

REE	139La	140Ce	141Pr	146Nd	147Sm	153Eu	157Gd	159Tb	163Dy	165Ho	166Er	169Tm	172Yb	175Lu
NBP95R10 Mean	40	21	6.4	23	4.8	1.5	6.4	1.2	8.7	2.3	7.4	1.2	8.3	1.6
1σ	6.5	3.5	0.84	3.1	1.18	0.29	0.80	0.24	1.28	0.40	0.79	0.22	0.94	0.30
Blank	1.9	6.1	0.6	1.4	0.8	0.2	0.5	0.05	0.21	0.09	0.17	0.06	0.14	0.08
PAAS	38	80	8.9	32	5.6	1.1	4.7	0.77	4.4	1	2.9	0.4	2.8	0.43

Supplemental Table DR2: REE concentrations for in-house consistency standard NBP95R10, standard deviation for NBP95R10, 1% HNO_3 blank, and PAAS. All measured values are pM (mean, 1σ, and blank); PAAS is reported in ppm.

REE patterns typically display increasing HREE enrichment with increasing water

depth in the ocean (e.g. Elderfield and Greaves, 1982; Klinkhammer et al., 1983;

Piepgras and Jacobsen, 1992; German et al., 1995; Abbott et al., 2015a). However,

this trend is not clearly observed in the Tasman Sea (Supplemental Figure DR4). At the southern station (CTD23) where water column neodymium concentrations are generally lower, we observe the greatest REE enrichment in the mid water column. The most HREE enriched waters at CTD23 were found between 1000 m and 2000 m and moderate HREE enrichment was observed between 2000 and 3000 m (Supplemental Figure DR4). The REE patterns in the seawater at CTD23 from <1000 m is most similar to the patterns in the seawater from >3000 m, with seawater in both of these regions showing a less HREE enriched pattern than observed in the mid-water column. Bottom water had one of the least HREE enriched patterns at both CTD sites. Any trend in REE pattern with water depth is less detectable at the northern site

(CTD54). This variability in REE patterns at CTD54 may be due to the non-conservative addition of REEs from a sedimentary source. The Nd concentrations in the AAIW and CDW at CTD54 are nearly double the Nd concentrations in the AAIW and CDW at CTD23 (main text Figure 3) supporting the need for an additional neodymium source as the water masses move through the Tasman Sea. The REE patterns of the water below 3000 m are the least HREE enriched, and are even less HREE enriched at CTD54 than at CTD23. The REE patterns between 2000 and 3000 m are also generally less HREE enriched at CTD54 than at CTD23. Surface waters (<1000 m) and those between 1000 and 2000 m are more variable at CTD54 than at CTD23, with some surface waters displaying HREE enrichment and some waters from >1000 m being relatively HREE depleted (Supplemental Figure DR4). CTD54 water column REE patterns are overall slightly less HREE enriched than those observed at CTD23 for water between 1000 and 3000 m at CTD54.

The deepest waters (>3000 m) are the best indicator of benthic processes influencing the water mass between CTD 23 and CTD 54 because they most represent the northward flowing CDW and are less influenced by the multi-directional flow of the AAIW (main text Figure 1) or local surface water inputs (main text Figure 4). Interestingly, the REE patterns from water shallower than 1000 m are similarly HREE depleted to the bottom water at CTD23. Conversely, the shallower than 1000 m seawater REE patterns at CTD54 are more HREE enriched than the corresponding deep waters. The similarity between the upper most water column and the bottom waters at CTD24 could indicate reversible scavenging is transferring REE from the shallow to deep ocean as previously proposed (e.g. Elderfield, 1988; Byrne and Kim, 1990; Sholkovitz et al., 1994; Byrne and Sholkovitz, 1996). However, the similarity between the upper most water column and the bottom waters could also be interpreted to indicate a particulate source of REEs to the surface waters (e.g. Jeandel and Oelkers, 2015, Rousseau et al., 2015) that has a similar REE pattern to that of a sedimentary source. I argue that together, the less HREE enriched REE pattern of deep water and the higher overall water column concentrations of neodymium at CTD54 relative to CTD23 favor the hypothesis of a benthic source of REEs to the CDW as this water mass moves through the Tasman Sea. The less HREE enriched REE patterns observed in the deepest waters are similar to the typical HREE pattern of published pore waters REE patterns (e.g. Elderfield and Sholkovitz, 1987; Sholkovitz et al., 1989; Haley et al., 2004; Schacht et al., 2010; Kim et al., 2012; Abbott et al., 2015a; Du et al., 2016; Haley et al., 2017). These less HREE enriched patterns were also observed in connection with benthic flux observations in the North Pacific (Abbott et al., 2015a) and supported by isotopic data (Abbott et al., 2015b).

The bottom water at both CTD locations had one of the least HREE enriched patterns

at both sites consistent with this benthic flux hypothesis.

Figure Captions

Supplemental Figure DR1: Computer rendering of the bathymetry at site CB2600 from multi-beam swath data collected on board RV *Investigator.*

Supplemental Figure DR2: Backscatter electron image of sediments from CB2600 showing large quartz (top right) and calcite (middle right) sediment grains characteristic of the site. A 40 μm scale bar is provided. Backscatter electron image from scanning electron microscope (SEM) analysis on an FEI Teneo LoVac field emission SEM equipped with dual Bruker XFlash Series 6 energy dispersive x-ray spectroscopy (EDS) detectors at Macquarie University.

Supplemental Figure DR3: Dissolved iron (orange diamonds), manganese (brown triangles), and phosphorous (pink circles) for sites PH150, JB1500, and CB2600. Iron and manganese concentrations are on the top x axis in ppb and phosphorous concentrations are on the bottom x axis in ppb.

Supplemental Figure DR4: Rare Earth Element patterns from CTD23 and CTD54. Patterns are color coded into one of 4 ranges based on water depth: 1) surface waters less than 1000 m (light blue squares), 2) 1000 – 2000 m water depth (dark blue circles), 3) 2000 – 3000 m water depth (purple diamonds), and 4) below 3000 m (solid black triangles). Bottom water is shown as white triangles with black lines. The negative Ce anomaly characteristic of seawater is visible in all samples. All REE concentrations have been normalised to PAAS and praseodymium concentrations.

Supplemental References

Abbott, A.N., Haley, B., McManus, J., and Reimers, C., 2015a, The sedimentary source of dissolved rare earth elements to the ocean: Geochimica et Cosmochimica Acta, v. 154, p. 186-2000, doi: 10.1016/j.gca.2015.01.010.

Abbott, A.N., Haley, B., and McManus, J., 2015b, Bottoms up: Sedimentary control of the deep North Pacific Ocean's ε_{Nd} Signature: Geology, v. 45, p. 1035-1038, doi: 10.1130/G37114.1

Akagi, T., 2013, Rare earth element (REE) silicic acid complexes in seawater to explain the incorporation of REEs in opal and the "leftover" REEs in surface water: new interpretation of dissolved REE distribution profiles: Geochimica et Cosmochimica Acta, 113, 174-192, doi: 10.1016/j.gca.2013.03.014.

Bertram, C.J., and Elderfield, H.,1993, The geochemical balance of the rare earth elements and neodymium isotopes in the ocean: Geochimica et Cosmochimica Acta, 57, 1957-1986, doi: 10.1016/0016-7037(93)90087-D.

Byrne, R.H., and Kim, K.-H., 1990, Rare earth element scavenging in seawater: Geochimica et Cosmochimica Acta, 54, 2645-2656, doi: 10.1016/0016-7037(90)90002-3.

Byrne, R.H., and Sholkovitz, E.R., 1996, Marine chemistry of the lanthanides: In *Handbook on the Physics and Chemistry of Rare Earths*, v. 23, p. 497-593, eds. Jr.K. A. Gschneider and L. Eyring, Elsevier.

Censi, P., Sprovieri, M., Saiano, F., Di Geronimo, S.I., Larocca, D., and Placenti, F., 2007, The behaviour of REEs in Thailand's Mae Klong estuary: Suggestions from the Y/Ho ratios and lanthanide tetrad effects: Estuarine, Coastal, and Shelf Science, v. 71, p. 569-579, doi: 10.1016/j.ecss.2006.09.003

Du, J., Haley, B.A., and Mix, A.C., 2016, Neodymium isotopes in authigenic phases, bottom waters and detrital sediments in the Gulf of Alaska and their implications for paleo-circulation reconstruction: Geochimica et Cosmochimica Acta, v. 193, p. 14-35, doi: 10.1016/j.gca.2016.08.005.

Elderfield, H., and Greaves, M.J.,1982, The rare earth elements in seawater. Nature, v. 296, p. 214-219.

Elderfield, H., and Sholkovitz, E.R., 1987, Rare earth elements in the pore waters of reducing nearshore sediments: Earth and Planetary Science Letters, v. 82, p. 280-288, doi: 10.1016/0012-821X(87)90202-0.

Elderfield, H., 1988, The oceanic chemistry of the rare-earth elements: Philosophical Transactions of the Royal Society of London, 325, 105-126, doi: 101098/rsta.1988.0046.

German, C.R., Masuzawa, T., Greaves, M.J., Elderfield, H., and Edmond, J.M., 1995, Dissolved rare earth elements in the Southern Ocean: Cerium oxidation and the influence of hydrography: Geochimica et Cosmochimica Acta, 59, 1551-1558, doi: 10.1016/0016-7037(95)00061-4.

Goldberg, E.D., Koide, M., Schmitt, R.A., and Smith, R.H. (1963) Rare earth distributions in the marine environment: Journal of Geophysical Research, v. 68, p. 4209-4217.

Haley, B.A., Klinkhammer, G., and McManus, J., 2004, Rare earth elements in pore waters of marine sediments: Geochimica et Cosmochimica Acta, v. 68, p. 1265-1279, doi: 10.1016/j.gca.2003.09.012

Haley, B.A., Du, J., Abbott, A.N., and McManus, J., 2017, The Impact of Benthic Processes on Rare Earth Element and Neodymium Isotope Distributions in the Oceans: Frontiers in Marine Science, v. 4, art. 426, doi: 10.3389/fmars.2017.00426.

Jeandel, C., and Oelkers, E.H., 2015, The influence of terrigenous particulate material dissolution on ocean chemistry and global element cycles: Chemical Geology, v. 395, p. 50-66, doi: 10.1016/j.chemgeo.2014.12.001.

Kim, J., Torres, M.E., Haley, B.A., Kastner, M., Pohlman, J.W., Riedel, M., and Lee, Y.-J., 2012, The effect of diagenesis and fluid migration on rare earth element distribution in pore fluids of the northern Cascadia accretionary margin: Chemical Geology, v. 291, p. 152-165, doi: 10.1016/j.chemgeo.2011.10.010

Klinkhammer G., Elderfield, H., and Hudson, A., 1983, Rare earth elements in seawater near hydrothermal vents: Nature, v. 305, p. 185-188.

Kuss, J., Garbe-Schonberg, C.D., and Kremling, K., 2001, Rare earth elements in suspended particulate material of North Atlantic surface waters: Geochimica et Cosmochimica Acta, v. 65, p. 187-199, doi: 10.1016/S0016-7037(00)00518-4

Lacan, F., and Jeandel, C., 2005, Neodymium isotopes as a new tool for quantifying exchange fluxes at the continent-ocean interface: Earth and Planetary Letters, v. 232, p. 245-257, doi 10.1016/j.epsl.2005.01.004

Nozaki, Y., and Alibo, D.S., 2003, Importance of vertical geochemical processes in controlling the oceanic profiles of dissolved rare earth elements in the northeastern Indian Ocean: Earth and Planetary Science Letters, 205, 155-172, doi: 10.1016/S0012-821X(02)01027-0

Piepgras, D.J., and Jacobsen, D.B., 1992, The behavior of rare earth elements in seawater: Precise determination of variations in the North Pacific water column: Geochimica et Cosmochimica Acta, v. 56, p.1851-1862, doi:10.1016/0016-7037(92)90315-A.

Rousseau, T.C.C., Sonke, J.E., Chmeleff, J., van Beek, P., Souhaut, M., and Boaventura, G., 2015, Rapid neodymium release to marine waters from lithogenic sediments in the Amazon estuary: Nature Communications, 6, doi: 10.1038/ncomms8592.

Schacht, U., Wallman, J., and Kutterolf, S., 2010, The influence of volcanic ash alteration on the REE composition of marine pore waters: Journal of Geochemical Exploration, v. 106, p. 176-187, doi: 10.1016/j.gexplo.2010.02.006
Schmidt, S., and De Deckker, P., 2015, Present-day sedimentation rates on the southern and southeastern Australian continental margins: Australian Journal of Earth Sciences, v. 62, p. 143-150, doi: 10.1080/08120099.2015.1014846.

Sholkovitz, E.R., Piepgras, D.J., and Jacobsen, S.B., 1989, The pore water chemistry of rare earth elements in Buzzards Bay sediments: Geochimica et Cosmochimica Acta, v. 53, p. 2847-2856, doi: 10.1016/0016-7037(89)9016202.

Sholkovitz, E.R., Landing, W.M., and Lewis, B.L., 1994, Ocean particle chemistry: the fractionation of rare earth elements between suspended particles and seawater: Geochimica et Cosmochimica Acta, 58, 1567-1579, doi: 10.1016/0016-7037(94)90559-2.
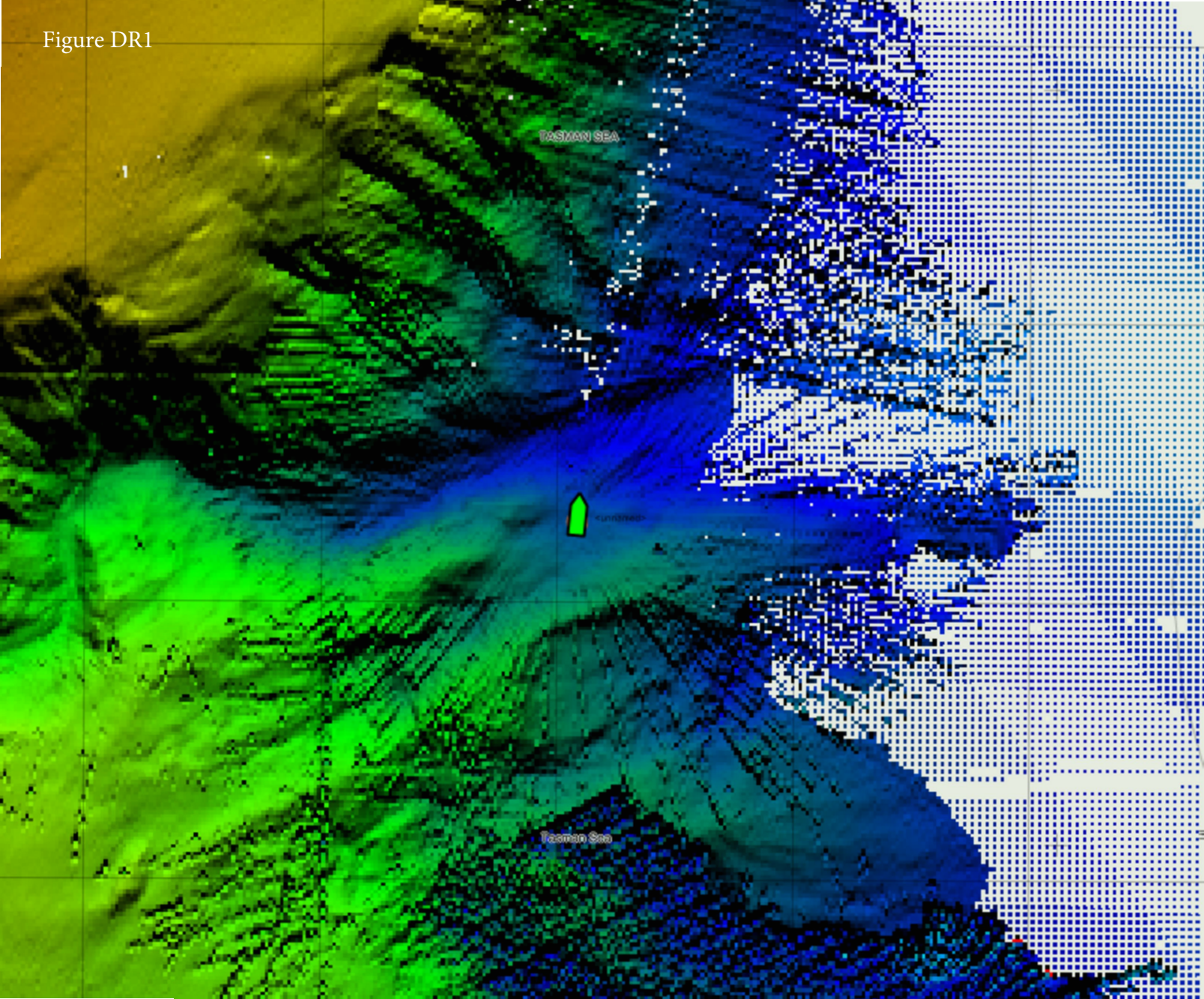
Taylor, S.R., and McLennan, S.M. (1985) The continental crust: its composition and evolution. An examination of the geochemical record preserved in sedimentary rocks. Blackwell Scientific Publications, Oxford.

Turner, D.R., Whitfield, M., and Dickson, A.G. (1981) The equilibrium speciation of dissolved components in freshwater and seawater at 25°C and 1 atm pressure. *Geochimica et Cosmochimica Acta*, v. 45, p. 855-881.
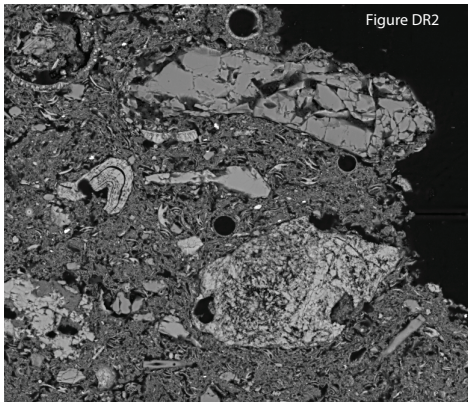
von Blanckenburg, F., 1999, Tracing Past Ocean Circulation? Science, v. 286, p. 1862-1863, doi: 10.1126/science.286.5446.1862b

Yang, J., and Haley, B., 2016, The profile of the rare earth elements in the Canada Basin, Arctic Ocean: Geochemistry, Geophysics, Geosystems, v.17, p. 3241-3253, doi: 10.1002/2016gc006412
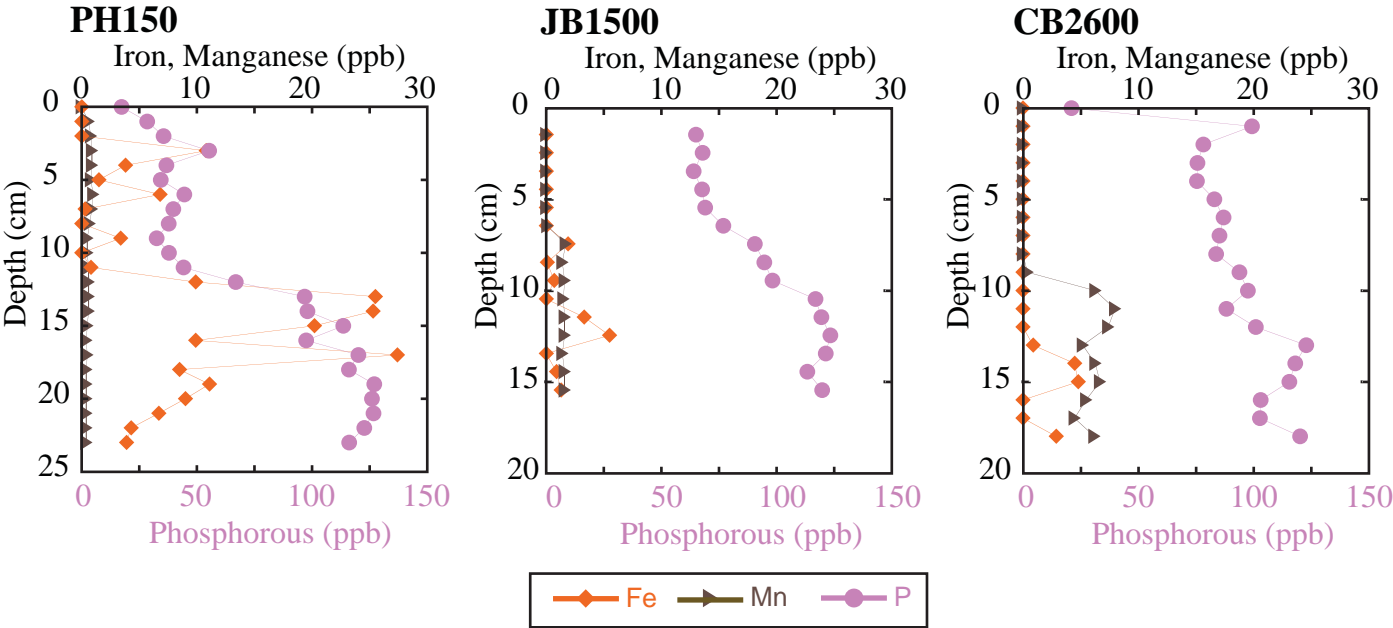
Figure DR1

CB2600

Figure DR2

⊢——⊣ 40μm

Figure DR3

Figure DR4